J Biomol NMR (2013) 55:219–223
DOI 10.1007/s10858-012-9695-5

NMR STRUCTURE NOTE

Solution structure of the *Magnaporthe oryzae* avirulence protein AvrPiz-t

Zhi-Min Zhang · Xu Zhang · Zi-Ren Zhou · Hong-Yu Hu · Maili Liu · Bo Zhou · Jiahai Zhou

Received: 11 November 2012 / Accepted: 6 December 2012 / Published online: 20 January 2013
© Springer Science+Business Media Dordrecht 2013

Biological context

Plants have evolved two major layers of defense mechanisms against invasion by diverse pathogens. When host membranes are exposed to pathogens, plants use extracellular surface receptors to identify pathogen-associated molecular patterns (PAMPs) and initiate so-called PAMP-triggered immunity (PTI) (Chisholm et al. 2006). Once pathogens gain hold in plants by suppressing this primary defense, plants express cytoplasmic resistance proteins that recognize pathogen-derived effector proteins and mount a more specialized defense mechanism referred to as effector-triggered immunity (ETI, Chisholm et al. 2006). To enable parasitism, pathogens usually use an arsenal of effector proteins that are delivered into plant cells to exert their primary function of interfering with the host immunity (Abramovitch et al. 2006; Feng et al. 2012; Wilton et al. 2010). However, effector proteins in some cases act as traitors by inducing effector-triggered immunity; these proteins are often referred to as avirulence proteins (Jones and Dangl 2006). Despite unparalleled progress in the identification of a vast repertoire of putative effectors in diverse pathogens in the last decade, the biochemical basis for the vast majority of those effectors remains unknown.

The interaction between rice and the fungal pathogen *Magnaporthe oryzae*, the causal agent of the devastating rice blast disease, observes the gene-for-gene model. The rice blast resistance gene *Piz-t* and the *M. oryzae* avirulence gene *AvrPiz-t* were successively isolated by map-based cloning methods (Zhou et al. 2006; Li et al. 2009). Co-expression of the pair of Piz-t/AvrPiz-t mounts effective immunity in rice (Li et al. 2009). The *AvrPiz-t* gene encodes a small protein predicted to be secreted that shows no homology to known proteins and is 108 amino acids in length (Li et al. 2009). *AvrPiz-t* can suppress programmed cell death (PCD) induced by BAX in tobacco, suggesting that it might contribute to the pathogenicity of *M. oryzae* (Li et al. 2009). Recently, Park et al. (2012) demonstrated that ectopic expression of *AvrPiz-t* gene in rice leads to reduced response of ROS triggered by flg22 and chitin, and enhanced susceptibility to the virulent rice blast strain. These data suggested that AvrPiz-t functions primarily as a

Zhi-Min Zhang and Xu Zhang contributed equally to the present work.

Electronic supplementary material The online version of this article (doi:10.1007/s10858-012-9695-5) contains supplementary material, which is available to authorized users.

Z.-M. Zhang · J. Zhou (✉)
State Key Laboratory of Bio-organic and Natural Products Chemistry, Shanghai Institute of Organic Chemistry, Chinese Academy of Sciences, 345 Lingling Road, Shanghai 200032, China
e-mail: jiahai@mail.sioc.ac.cn

X. Zhang · M. Liu
Wuhan Center for Magnetic Resonance, State Key Laboratory of Magnetic Resonance and Atomic and Molecular Physics, Wuhan Institute of Physics and Mathematics, Chinese Academy of Sciences, Wuhan 430071, China

Z.-R. Zhou · H.-Y. Hu
State Key Laboratory of Molecular Biology, Institute of Biochemistry and Cell Biology, Shanghai Institutes for Biological Sciences, Chinese Academy of Sciences, Shanghai 200031, China

B. Zhou (✉)
State Key Laboratory Breeding Base for Zhejiang Sustainable Pest and Disease Control, Institute of Virology and Biotechnology, Zhejiang Academy of Agricultural Sciences, Hangzhou 310021, China
e-mail: b.zhou@irri.org

virulence effector contributing to the pathogenicity of *M. oryzae*. To further understand the mechanism of the pathogenicity-associated function of *AvrPiz-t*, we determined its solution structure.

Methods and results

Protein expression and purification

Full-length AvrPiz-t contains an 18-residue signal peptide at its N-terminus. A DNA fragment encoding the mature protein (residues 19–108) was amplified from pGEX-AvrPiz-t by PCR with Phanta™ Super-Fidelity DNA polymerase (Vazyme Biotech, China) and the following primers: 5′-AGACGGATCCAGCTTCGTACAATGCAATCATCATC-3′ and 5′-ATGCAAGCTTCTATTGGCGCTGAGCCTGAG-3′. The PCR products were digested with *Bam*HI/*Hin*dIII and ligated into the correspondingly digested ppSUMO vector (a gift from Prof. Ming Lei, University of Michigan, Ann Arbor, MI, USA). The SUMO-fused AvrPiz-t protein was expressed with an N-terminal hexahistidine in *Escherichia coli* BL21 (DE3). Transformed cells were grown in LB medium at 37 °C and induced by adding isopropyl-thio-β-D-galactoside to a final concentration of 0.4 mM when the cell density reached an OD_{600} of 1.0. The cells were incubated at 16 °C for a further 6 h before harvesting by centrifugation for 10 min at 4 °C and 5,000×*g*. For ^{15}N and ^{13}C labeling, expression was carried out using *E. coli* Rosetta (DE3) cells in M9 minimal medium.

Cell pellets were resuspended in 50 mL lysis buffer (25 mM Tris, pH 8.0, 200 mM NaCl, 5 mM β-mercaptoethanol) and lysed by sonication. The supernatant was centrifuged for 30 min at 4 °C and 100,000×*g*. The soluble fractions were applied to a 5 mL Ni^{2+}–NTA column (GE Healthcare, Fairfield, USA) equilibrated with lysis buffer. The His-tagged SUMO AvrPiz-t fusion protein was eluted from the affinity column with lysis buffer containing 250 mM imidazole, and subjected to ULP1 protease digestion overnight at 4 °C. The cleaved His-tagged SUMO protein, undigested AvrPiz-t protein samples and the His-tagged ULP1 protease were removed using a second nickel affinity chromatography step. Proteins from the flow through were pooled and further purified by Resource S ion exchange chromatography (GE Healthcare) and gel filtration using a Superdex 75 16/60 column (GE Healthcare). The purified AvrPiz-t proteins were stored in 20 mM sodium phosphate, pH 6.5 and 50 mM NaCl.

SDS-PAGE analysis showed that AvrPiz-t underwent a slow single-step cleavage during purification and storage to give a stable fragment with a molecular weight similar to that of the intact protein. Decreasing the temperature or changing the buffer components was ineffective for preventing the protein from degrading. The purified recombinant proteins degraded completely to the stable fragments in 3 days at room temperature. The degraded products, however, were stable for more than 3 weeks at room temperature. The N-terminal amino acid residue sequence of the stable fragment was determined as SFV by the Edman degradation method on an Applied Biosystems 491 Protein sequencer. This suggested that the N-terminus of AvrPiz-t was the same as the original protein and that the degradation happened at the C-terminus. The molecular weight of the stable fragment was determined by LC–MS to be 8,729, 1,116.1 Da smaller than the theoretic molecular weight (9,845.1 Da) of the intact protein (Supplemental Fig. 1). Based on the amino acid sequence of AvrPiz-t, we deduced that the last 10 residues (residues 99–108, IGNDPQAQRQ) of the full-length protein were missing from the stable fragment. As estimated by SDS-PAGE, the purity of the fragment was more than 95 % with no prominent contaminant, so we decided to determine the solution structure of this core region of AvrPiz-t.

The NMR samples were prepared by dissolving either ^{15}N-enriched or ^{15}N and ^{13}C dually labeled AvrPiz-t (0.3 mM) in 20 mM sodium phosphate (pH 6.5), 50 mM NaCl, 0.2 % sodium azide, 10 % D_2O. For H/D exchange experiments, a ^{15}N labeled sample stored in the same buffer was lyophilized and then dissolved in D_2O.

NMR measurements

NMR data for structure calculation and H/D exchange were collected at 293 K on Avance-800 (Bruker) and Inova-600 (Varian) spectrometers equipped with z-gradient triple-resonance cryo-probes. Two-dimensional (2D) ^{15}N-edited TROSY and three-dimensional (3D) CBCA(CO)NH, HNCACB, HNCO, HN(CO)CA, HNCA and HCCH-TOCSY experiments were performed for the backbone and aliphatic side chain resonance assignments. A combination of (Hβ)Cβ(CγCδ)Hδ, (Hβ)Cβ(CγCδCε)Hε, and NOE experiments were employed for the resonance assignment of aromatic side chains. 3D ^{15}N- and ^{13}C-edited NOESY-HSQC spectra were collected to confirm the chemical shift assignments and generate distance restraints for structure calculations. All NMR spectra were processed with NMRPipe (Delaglio et al. 1995) and analyzed using Sparky (Goddard and Kneller, SPARKY 3).

Structure calculation

The solution structures of AvrPiz-t were determined based on 729 NOE-derived distance restraints, 89 backbone dihedral angle restraints, 22 hydrogen bond restraints, and one disulfide bond restraint (Table 1). No disulfide bond restraints were used for the initial structure calculation.

Table 1 Structural statistics of the final 20 energy-minimized AvrPiz-t conformers

NOE-derived distance restraints	729
Intra-residue	306
Sequential ($\|i - j\| = 1$)	193
Medium-range ($1 < \|i - j\| < 5$)	40
Long-range ($\|i - j\| > 5$)	190
Number of H-bond restraints	22
Number of dihedral angle restraints	
φ	45
Ψ	44
Ramachandran plot (%)	
Most favored regions	78.2
Additionally allowed regions	17.1
Generously allowed regions	1.27
Disallowed regions	3.38
RMSD from mean (residues 21–90) (Å)	
Backbone atoms	0.72 ± 0.19
All heavy atoms	1.23 ± 0.20

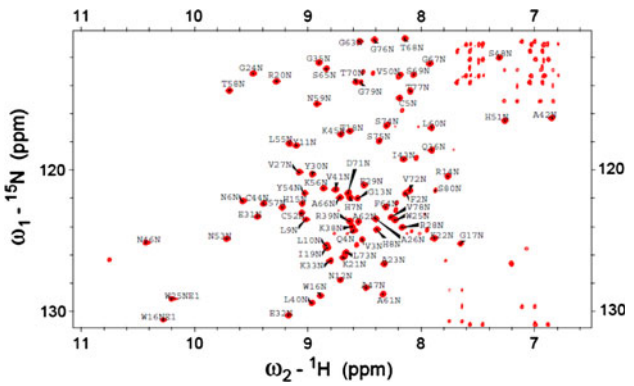

Fig. 1 ^{1}H–^{15}N TROSY spectrum of AvrPiz-t with sequence-specific assignments. The spectrum was recorded at 800 MHz and 293 K. Backbone amide correlations are indicated by one-letter amino acid code followed by residue number and N. The resonances of the tryptophan indole groups are specifically labeled with one-letter amino acid code followed by NE1. The resonances of the side chain NH_2 groups were not assigned

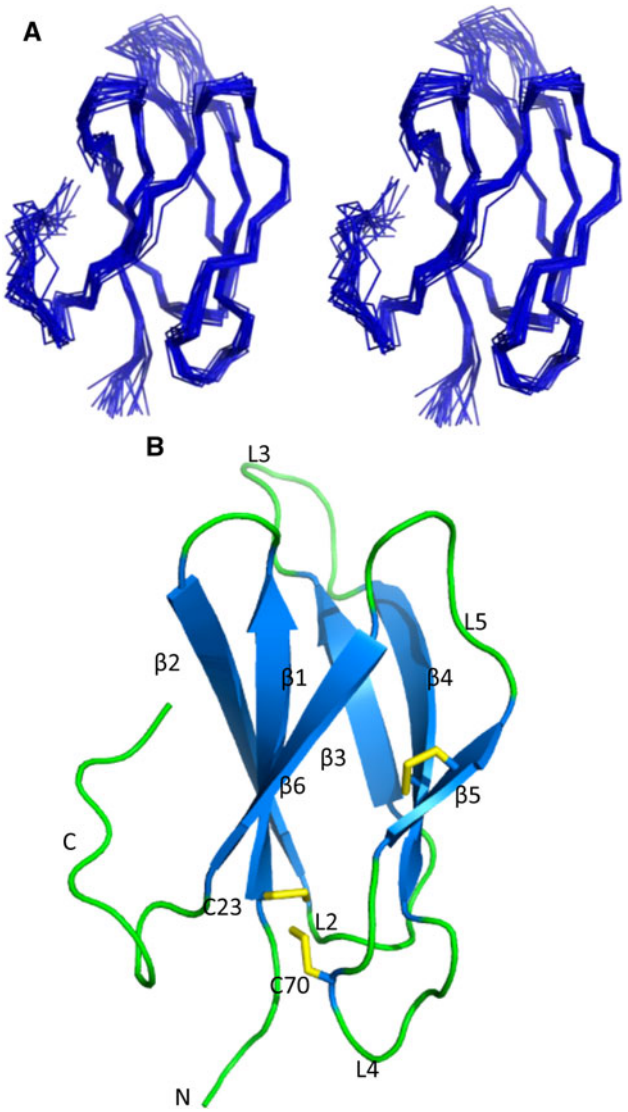

Fig. 2 Solution structure of AvrPiz-t. **a** Ensemble of 20 selected conformers with lowest energy. **b** Ribbon representation of the final structure in which the N- and C-termini as well as the secondary structure elements are indicated. The β-strands are colored in cyan, while the loops are drawn in *green*. The side chains of four cysteine residues are depicted as *yellow sticks*

Hydrogen bond restraints (two per hydrogen bond) were generated by a combination of H/D exchange data, medium-range NOEs, and secondary structural information using the program CSI (Wishart and Sykes 1994). The backbone dihedral angle restraints were generated with TALOS (Cornilescu et al. 1999). Structures were calculated using ARIA (Rieping et al. 2007) and refined using CNS (Brunger et al. 1998). Nine cycles of iterative NOE peak assignments were employed for the structure refinement. Two hundred structures were calculated and the 20 best conformers with the lowest energies, which exhibited no obvious NOE violations and no dihedral violations >5 Å, were selected for final analysis (Table 1). The quality of the structures was analyzed using PROCHECK-NMR (Laskowski et al. 1996) and CNS. The Dali server (Holm and Sander 1993) was used to search for structurally similar proteins.

Spectral analysis

The assigned ^{1}H,^{15}N-TROSY spectrum was well dispersed as illustrated in Fig. 1. Backbone assignments were essentially complete except the amide nitrogen of the

N-terminal Ser19. A number of side chain resonance assignments were missing, most of which belonged to the C-terminal residues (residues 91–98). A few resonances could be assigned only with the help of NOEs after initial structure calculations. A total of 907 NOE cross-peaks were integrated, resulting in 729 meaningful distance restraints. The NOE connectivity pattern between the backbone protons was used to determine the secondary structure elements of the protein. A large number of strong sequential dαN(i, i + 1) NOE correlations indicated predominantly β-strand elements, which was consistent with the predicted result using the program CSI. With the help of TALOS, it was possible to obtain 44 pairs of backbone (φ, ψ) dihedral angle restraints. Twenty-two hydrogen bond restraints (two per hydrogen bond) were generated by a combination of H/D exchange data, medium-range NOEs, and chemical shift index.

Structural features of AvrPiz-t

The atomic coordinates and NMR-derived restraints of AvrPiz-t have been deposited in the Protein Data Bank (http://www.pdb.org/) under accession code 2lw6. The chemical shift assignments of ECRG2 have been deposited in the Biological Magnetic Resonance Data Bank (http://www.bmrb.wisc.edu/) with accession number 18607. Figure 2 shows the superposition of backbone traces of the final 20 energy-minimized AvrPiz-t conformers. The root-mean-square deviation (r.m.s.d) for backbone heavy atoms in regular secondary elements (residues 21–90) was 0.72 ± 0.19 and 1.23 ± 0.20 Å for all heavy atoms.

Residues 22–90 of AvrPiz-t form a six-strand β-sandwich structure while the extreme N-terminus (residues 19–21) and C-terminus (residues 91–98) are disordered (Fig. 2). The conformation of the two termini is uncertain because NMR structural calculation of these parts lacks long-range distance restraints. The core structure contains two antiparallel β-sheets packed face-to-face and connected by loop 2 (residues 40–44) and loop 5 (residues 77–81). Each sheet is formed by three β-strands: sheet I is composed of strands β1 (residues 23–29), β2 (residues 32–39) and β6 (residues 82–88) while sheet II contains β3 (residues 45–50), β4 (residues 57–64) and β5 (residues 73–76) (Fig. 2b). In sheet II, a disulfide bond between residues Cys62-Cys75 links strands β4 and β5. Two other cysteine residues Cys23 and Cys70, located on strand β1 and loop 4, respectively, are close to each other but do not form a disulfide bond (Fig. 2b).

Discussion and conclusions

The overall structure of AvrPiz-t adopts a six-strand β-sandwich fold. In the solution structure of AvrPiz-t, Cys62 forms a disulfide bond with Cys75. Cys23 and Cys70 are in the reduced cysteine form. Two AvrPiz-t derivatives that each contain a single amino acid mutation (cysteine to alanine) at these two cysteine residues were found to gain virulence, indicating that the disulfide bond C62–C75 could be important for the fulfillment of its avirulence function (Li et al. 2012).

Structural similarity searches of the Protein Data Bank were performed using the Dali server, but no homologous

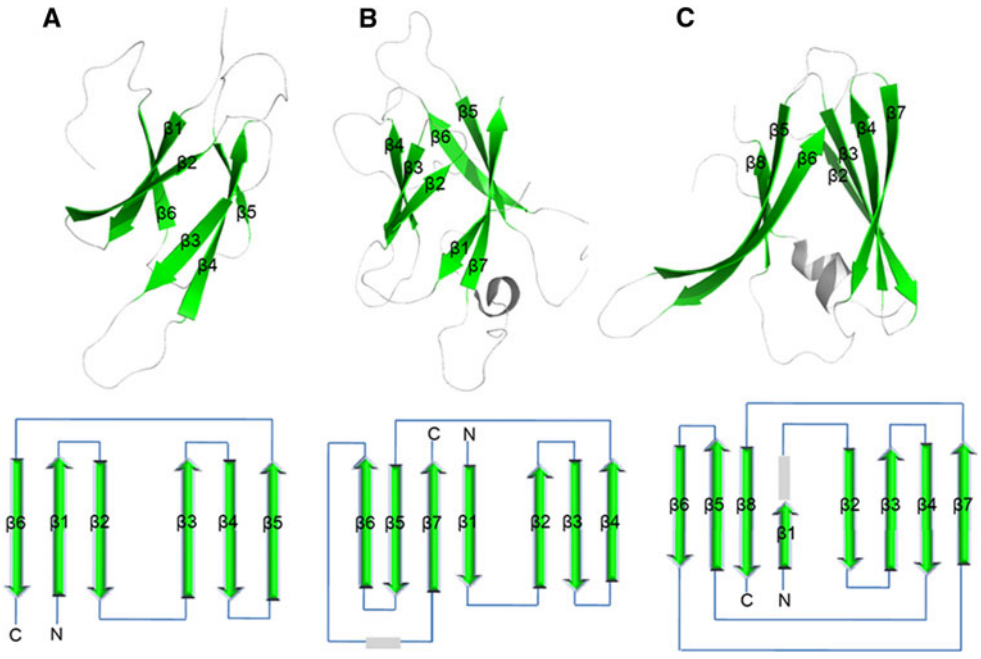

Fig. 3 Structure comparison of AvrPiz-t with AvrL567 and ToxA. **a** The ribbon and topology diagrams of AvrPiz-t. **b** The ribbon and topology diagrams of AvrL567 (PDB ID code 2QVT). **c** The ribbon and topology diagrams of ToxA (PDB ID code 1ZLD). The β-strands are colored in *green*, while the helices and loops are shown in *grey*

structures were found. The highest DALI Z scores were 3.1 and 2.9, with RMSDs of 3.9 and 3.1, respectively. Although there is no significant sequence similarity between AvrPiz-t and any other protein with its structure deposited, we found the β-sandwich fold does exist in other avirulence protein structures (Fig. 3). For example, the crystal structure of Flax rust (*Melampsora lini*) AvrL567 is a β-sandwich packed with one sheet of four antiparallel β-strands and the other sheet of three β-strands (Gunčar et al. 2007). The crystal structure of *P. tritici-repentis* ToxA has a similar β-sandwich fold with two antiparallel β-sheets composed of four strands each (Sarma et al. 2005). The structural similarities suggest that these proteins may share common elements in their mechanisms of uptake and recognition by their cognate R proteins.

We have identified 12 potential host targets of AvrPiz-t, designated as APIPs, from rice using a yeast two hybridization (Y2H) method (Zhou et al., unpublished). Interestingly, four proteins, APIP2, APIP6, APIP8 and APIP10, are likely to be involved in the ubiquitin proteasome system. More recently, Park et al. (2012) demonstrated that AvrPiz-t is ubiquitinated by APIP6 and suppresses the E3 ubiquitin ligase activity of APIP6 in vitro. Interestingly, AvrPiz-t and APIP6 promote the degradation of each other in plant cells (Park et al. 2012). Elucidating the structure of the AvrPiz-t/APIP6 complex will be crucial for understanding the mechanisms by which fungal effector proteins degrade the host E3 ligase to suppress PAMP-triggered immunity in rice.

Acknowledgments This work was supported by grants from the National Program on Key Basic Research of China (2009CB918600, to J. Z. and M. L.), the National Grand Project for Medicine Innovation (2011ZX09506-001) and the Natural Science Foundation in China (30971878, to B. Z.). We are grateful to Prof. Chunyang Cao and Yan Zhang for valuable suggestions in NMR structure determination. We also thank Dr. Wenyu Wen for her help on H/D exchange experiments.

References

Abramovitch RB, Janjusevic R, Stebbins CE, Martin GR (2006) Type III effector AvrPtoB requires intrinsic E3 ubiquitin ligase activity to suppress plant cell death and immunity. Proc Natl Acad Sci USA 103:2851–2856

Brunger AT, Adams PD, Clore GM, DeLano WL, Gros P, Grosse-Kunstleve RW, Jiang J-S, Kuszewski J, Nilges M, Pannu NS, Read RJ, Rice LM, Simonson T, Warren GL (1998) Crystallography & NMR system: a new software suite for macromolecular structure determination. Acta Crystallogr Sect D 54:905–921

Chisholm ST, Coaker G, Day B, Staskawicz BJ (2006) Host–microbe interactions: shaping the evolution of the plant immune response. Cell 124:803–814

Cornilescu G, Delaglio F, Bax A (1999) Protein backbone angle restraints from searching a database for chemical shift and sequence homology. J Biomol NMR 13:289–302

Delaglio F, Grzesiek S, Vuister GW, Zhu G, Pfeifer J, Bax A (1995) NMRPipe: a multidimensional spectral processing system based on UNIX pipes. J Biomol NMR 6:277–293

Feng F, Yang F, Rong W, Wu X, Zhang J, Chen S, He C, Zhou J-M (2012) A Xanthomonas uridine 5′-monophosphate transferase inhibits plant immune kinases. Nature 485:114–120

Gunčar G, Wang C-IA, Forwood JK, The T, Catanzariti A-M, Lawrence GJ, Loughlin FE, Mackay JP, Schirra HJ, Anderson PA, Ellis JG, Dodds PN, Kobe B (2007) Adaptive evolution has targeted the C-terminal domain of the RXLR effectors of plant pathogenic oomycetes. Plant Cell 19:2898–2912

Holm L, Sander C (1993) Protein structure comparison by alignment of distance matrices. J Mol Biol 233:123–138

Jones JDG, Dangl JL (2006) The plant immune system. Nature 444: 323–329

Laskowski RA, Rullmann JAC, MacArthur MW, Kaptein R, Thornton JM (1996) AQUA and PROCHECK-NMR: programs for checking the quality of protein structures solved by NMR. J Biomol NMR 8:477–486

Li W, Wang B, Wu J, Lu G, Hu Y, Zhang X, Zhang Z, Zhao Q, Feng Q, Zhang H, Wang Z, Wang G, Hna B, Wang Z, Zhou B (2009) The *Magnaporthe oryzae* avirulence gene AvrPiz-t encodes a predicted secreted protein that triggers the immunity in rice mediated by the blast resistance gene Piz-t. Mol Plant Microbe Interact 22:411–420

Li P, Dong B, Zhou H, Zhou B (2012) Functional analysis of cysteine residues of the *Magnaporthe oryzae* avirulence protein AvrPiz-t. Acta Phytopathologica Sinica 42:474–479

Park C-H, Chen S, Shirsekar G, Zhou B, Khang CH, Songkumarn P, Ning Y, Bellizzi M, Valent B, Wang G-L (2012) The *Magnaporthe oryzae* effector AvrPiz-t targets the RING E3 ubiquitin ligase APIP6 to suppress pathogen-associated molecular pattern-triggered immunity in rice. Plant Cell. doi:10.1105/tpc.112.105429

Rieping W, Habeck M, Bardiaux B, Bernard A, Malliavin TE, Nilges M (2007) ARIA2: automated NOE assignment and data integration in NMR structure. Bioinformatics 23:318–382

Sarma GN, Manning VA, Ciuffetti LM, Karplus PA (2005) Structure of Ptr ToxA: an RGD-containing host-selective toxin from *Pyrenophora tritici-repentis*. Plant Cell 17:3190–3202

Wilton M, Subramaniam R, Elmore J, Gelsensteiner C, Coaker G, Desveaux D (2010) The type III effector HopF2Pto targets Arabidopsis RIN4 protein to promote *Pseudomonas syringae* virulence. Proc Natl Acad Sci USA 107:2349–2354

Wishart DS, Sykes BD (1994) The 13C Chemical-shift index: a simple method for the identification of protein secondary structure using 13C chemical-shift data. J Biomol NMR 4:171–180

Zhou B, Qu S, Liu G, Dolan M, Sakai H, Lu G, Bellizzi M, Wang G-L (2006) The eight amino-acid differences within three leucine-rich repeats between Pi2 and Piz-t resistance proteins determine the resistance specificity to Magnaporthe grisea. Mol Plant Microbe Interact 19:1216–1228